Extended mode coupling and simulations in cellular-automata fluids

Toyoaki Naitoh* and Matthieu H. Ernst
Institute for Theoretical Physics, University of Utrecht, P.O. Box 80006, 3508 TA Utrecht, The Netherlands

Martin A. van der Hoef and Daan Frenkel
FOM—Institute for Atomic and Molecular Physics, P.O. Box 41883, 1009 DB Amsterdam, The Netherlands
(Received 21 March 1991)

The velocity autocorrelation function (VACF) of lattice-gas cellular-automata fluids has been calculated by mode-coupling (MC) theory for finite systems, including sound modes, and compared with computer simulations on small ($N \simeq 10^3$) and large ($N \simeq 10^6$) two- and three-dimensional (3D) systems for reduced densities f ranging from 0.05 to 0.8. For times t up to $6t_0$ (mean free times) the simulated VACF agrees with Boltzmann relaxation. In 2D the agreement with MC theory is excellent for $t > 9t_0$ and has been tested over intervals of several acoustic traversal times. In 3D the agreement is still good, but sets in after much larger times ($150t_0$ at $f=0.1$ and $60t_0$ at $f=0.8$). However, there are disagreements in the smallest systems at the lowest densities, where the observed VACF at largest times is about 6% ($f=0.1$) and 9% ($f=0.05$) larger than the theoretical values.

I. INTRODUCTION

The velocity autocorrelation function (VACF) of a tagged particle has a fundamental significance in nonequilibrium statistical mechanics. Its time integral defines the self-diffusion coefficient through the Green-Kubo relation, and its decay exhibits short-time kinetic relaxation, conceivably an intermediate cage effect, and long-time hydrodynamic relaxation. This paper essentially focuses attention on the basic question of to what extent macroscopic hydrodynamic concepts, as implemented in mode-coupling (MC) theories, provide a valid description down to microscopic space and time scales.

The models on which these concepts are tested are one-, two-, and three-dimensional lattice-gas cellular-automata fluids (LGCA's), such as the two-dimensional Frisch-Hasslacher-Pomeau (FHP)–III model [1] and the quasi-three-dimensional face-centered hypercubic (FCHC) model [1]. The VACF in these systems has been obtained [2–4] with remarkable statistical accuracy using the *moment propagation method,* an algorithm that *exactly calculates the VACF of a tagged particle* over all possible trajectories, for a single initial configuration of the fluid particles. Furthermore, round off errors are absent in the time evolution of LGCA fluids. Statistical noise is only present in generating the initial configurations of the N fluid particles, where N is typically 10^3-10^6 in two-dimensional simulations, and exceeds 10^5 in three-dimensional ones.

The simulation results show excellent agreement with the asymptotic long-time tails of $t^{-d/2}$ predicted by mode-coupling theory for times larger than $20t_0$ with t_0 being the mean free time. Mode-coupling theory assumes that the long-time relaxation to equilibrium can be described through the decay of products of hydrodynamic modes [5,6]. In particular, the combination of a shear and a self-diffusion mode leads to the asymptotic tail of the VACF [3,4].

Erpenbeck and Wood [7,8] have adapted the mode-coupling theory of Ernst, Hauge, and van Leeuwen [9] to finite systems, and have shown that sound modes are of considerable importance. Following Erpenbeck and Wood, the mode-coupling theory will be extended (i) to include *all possible product of pairs of hydrodynamic modes* (also those yielding subleading asymptotic time behavior), and (ii) to obtain *finite-size corrections* by adapting mode-coupling theory to finite systems having a discrete set of allowed wave numbers, instead of a continuous range. This extended mode-coupling theory will be applied to d-dimensional LGCA's and compared with existing and new computer simulations.

In the papers [5,10,11] we have studied a cellular-automata (CA) fluid on a line by means of MC theory and computer simulations. We observed (i) that the VACF in finite one-dimensional systems approaches a *constant negative value* of $O(1/N)$ for times short compared to the acoustic traversal time t_a of the finite periodic systems; (ii) that the VACF only vanishes for times exceeding several multiples of t_a; and (iii) that the long-time decay of the VACF in the infinite system is exponential. rather than algebraic, with a relaxation time t_s differen. from the mean free time t_0. All observations on small and large systems have been explained quantitatively with the extended MC theory for finite systems.

This paper deals with the two- and three-dimensional fluid models and is the LGCA counterpart of the articles [7,8] on hard disks and hard spheres. Very recently, Dijkstra and van der Hoef [12] also performed computer simulations on the actual *four-dimensional* FCHC model, where they observed the $t^{-d/2}$ tail at several densities with a coefficient that is about 20% larger than predicted by MC theory.

The outlook of the paper is as follows. The following three sections contain theoretical considerations. Section II deals with the ensemble dependence of fluctuations, Sec. III with the extensions of MC theory, and Sec. IV with the interference effects from periodic boundary conditions. Section V and VI discuss the simulation results

for finite two- and three-dimensional systems. A conclusion is given in Sec. VII.

II. SUBTRACTED TIME CORRELATION FUNCTIONS

The diffusion coefficient of a tagged particle in a LGCA is given by

$$D=\sum_{t=1}^{\infty}\langle v_x(t)v_x(0)\rangle+\tfrac{1}{2}\langle v_x^2\rangle\equiv\langle v_x^2\rangle\left[\sum_{t=1}^{\infty}\phi(t)+\tfrac{1}{2}\right], \tag{2.1}$$

as follows by transforming Einstein's formula for the mean-square displacement. The VACF $\phi(t)=\langle v_x(t)v_x\rangle/\langle v_x^2\rangle$ should be considered in the thermodynamic limit.

In computer simulations, the normalized VACF, denoted by $\phi_{\mathrm{MD}}(t)$, is calculated using the molecular-dynamics (MD) ensemble, in which each system is contained in a periodic macroscopic box with V sites and has a fixed number of particles N, one of which is tagged ($N^*=1$), and *vanishing* total momentum, $\mathbf{P}=0$. The energy E is either trivially kept fixed in single speed models, where E and N are essentially the same, or it is not kept fixed at all because it is not conserved in the most commonly used lattice gases.

In theoretical calculations we use a canonical ensemble, in which the total momentum of each system fluctuates around an average $\langle\mathbf{P}\rangle=0$. Suppose a system has a finite total momentum $\mathbf{P}$, then the velocity of the tagged particle should be measured in the system's rest frame and the diffusion coefficient is given by Eq. (2.1) with $\mathbf{v}$ replaced by $\mathbf{v}'=\mathbf{v}-\mathbf{P}/N$. The corresponding *subtracted* VACF is defined as

$$\phi_N(t)=\langle v_x'(t)v_x'(0)\rangle/\langle v_x'^2\rangle\ . \tag{2.2}$$

From now on, the brackets $\langle\ \rangle$ without a subscript refer to a canonical average. As discussed more extensively in Ref. [10], subtracted correlation functions $\langle\delta\hat{A}(t)\delta\hat{B}(0)\rangle$ are physically the most relevant ones. The reasons are as follows. First, the Green-Kubo formulas for all transport coefficients, such as (2.1), are expressed in terms of them, as pointed out by Green [13]. Second, according to the theory of Lebowitz, Percus, and Verlet [14] on the ensemble dependence of fluctuations, subtracted fluctuation formulas, whether taken at equal or different times, are independent of the ensemble used for sufficiently large systems, whereas unsubtracted correlation functions $\langle\delta A(t)\delta B(0)\rangle$ are not. As shown in Ref. [10], $\phi_N(t)$ is a subtracted fluctuation formula in the sense of Refs. [13] and [14]. In the MD ensemble ($\mathbf{P}=0$), the tagged particle's velocity $\mathbf{v}=\mathbf{v}'$ is also a subtracted current. Therefore, the subtracted correlation function in the MD ensemble and that in (2.2) are expected to be equal, $\phi_{\mathrm{MD}}(t)=\phi_N(t)$, to terms of $O(1/N)$ included. The standard VACF of the canonical ensemble

$$\psi_N(t)=\langle v_x(t)v_x(0)\rangle/\langle v_x^2\rangle \tag{2.3}$$

and the subtracted one of Eq. (2.2) are related through

$$\psi_N(t)=\phi_N(t)+\frac{1-f}{N}\ . \tag{2.4}$$

This relation can be derived by using $\langle P_x^2\rangle=N(1-f)\langle v_x^2\rangle$, where the factor $(1-f)$ results from the Fermi exclusion rule. In the classical fluid of Refs. [7] and [8], $\langle P_x^2\rangle=N\langle v_x^2\rangle$. Here, $f=\rho/b$ denotes the reduced density ($0\le f\le 1$) and ρ and b are, respectively, the number of particles and velocity channels per site in the lattice.

In our theoretical and computer studies we shall be using periodic boundary conditions to minimize finite-size effects. Then subtracted correlation functions, such as $\phi_{\mathrm{MD}}(t)$ and $\phi_N(t)$, appearing in Green-Kubo relations, are supposedly vanishing at $t\to\infty$ at fixed numbers of particles N and sites V per macroscopic unit cell, because the subtracted fluctuations $\delta\hat{A}(t)$ have no component parallel to any conserved quantity. The unsubtracted VACF $\psi_N(t)$ contains a current $v_x(t)$ with an invariant component P_x/N and therefore approaches a *positive constant* $(1-f)/N$ in the same limit.

As will be explained in the following section, the constant correction term $(1-f)/N$ should be added to the simulation results $\phi_{\mathrm{MD}}(t)$ as a finite-size correction, in order to improve the agreement of the simulation results for different system sizes with those for the infinite system. In the analysis of Ref. [7], $\phi_{\mathrm{MD}}(t)$ is calculated in a microcanonical ensemble with ENV fixed, whereas $\phi_N(t)$ is calculated in a canonical ensemble with TNV fixed. Both correlation functions differ therefore by a term of $O(1/N)$. Such $1/N$ corrections are absent in the athermal LGCA's, considered here, because the energy E is not conserved and the models have no temperature.

III. EXTENDED MODE-COUPLING THEORY

Mode-coupling studies on the long-time behavior of the VACF have already been considered in Refs. [2–11]. In that case the current of tagged particles $\mathbf{v}$ in Eq. (2.3) is interpreted as the coarse-grained expression $\sum_{\mathbf{r}}u_x(\mathbf{r},t)P(\mathbf{r},t)$ with $u_x(\mathbf{r},t)$ the local fluid velocity and $P(\mathbf{r},t)$ the concentration of tagged particles. The time dependence of these slowly varying fields is calculated from the diffusion equation and the hydrodynamic equations, where the flow field is decomposed into shear modes and sound modes. By including sound modes in the considerations of Refs. [3–5], the expression for the VACF in finite systems is found to be

$$\begin{aligned}\psi_N(t)&\equiv\phi_N(t)+(1-f)/N\\&\equiv\frac{(1-f)}{N}\sum_{\mathbf{q}}\left[\left[\frac{d-1}{d}\right]\exp[-(D+\nu)q^2t]\right.\\&\qquad\left.+\frac{1}{d}\cos(c_0qt)\exp[-(D+\tfrac{1}{2}\Gamma)q^2t]\right],\end{aligned} \tag{3.1}$$

where D is the self-diffusion coefficient, $\Gamma=2(1-d^{-1})\nu+\zeta$ is the sound damping constant, and ν and ζ are the shear and bulk viscosity, respectively. The values of the transport coefficients depend, of course, on the col-

lision rules for the specific models and will be discussed in the specific applications.

The MC result (3.1) has been extended in two respects in comparison with existing theories.

(i) In addition to shear modes that yields the dominant $t^{-d/2}$ tails of [2–5], we have included sound modes yielding more rapidly decaying contributions to the VACF.

(ii) We have retained finite-size corrections, such as the $O(1/N)$ effect in Eq. (2.4) and the discrete $\mathbf{q}$ summation instead of a $\mathbf{q}$ integral.

Systems with periodic boundary conditions may be viewed as finite or infinite. In the former interpretation a position-dependent function $h(\mathbf{r})$ is only defined for $\mathbf{r}$ inside one macroscopic cell with $V=L^d$ sites. In Fourier space the $\mathbf{q}$ sums are restricted to the first Brillouin zone of the reciprocal lattice. In the latter interpretation one defines a position-dependent function as $H(\mathbf{r})=\sum_{l\in\mathcal{L}}h(\mathbf{r}+lL)$ with $\mathbf{r}$ in infinite space, which is periodic with period L in each space direction. The points l denote points of the regular infinite-space lattice $\mathcal{L}$ on which the LGCA is defined. In Fourier space, where $\mathbf{q}=2\pi\mathbf{n}/L$, the $\mathbf{q}$ summation extends over all points $\mathbf{n}$ of the corresponding infinite reciprocal lattice $\mathcal{L}^*$.

The result for $\psi_N(t)$ or $\langle v_x(t)v_x(0)\rangle$ is very similar to the finite N results of Ref. [7]. The only difference is actually the overall factor $(1-f)$ in the second line of Eq. (3.1), which results from the Fermi exclusion rule for the lattice-gas particles. We observe, furthermore, that the time-independent term ($\mathbf{q}=0$) in Eq. (3.1) yields the *constant* contribution $(1-f)/N$. Consequently, the MC result for the *subtracted correlation function*, $\phi_N(t)$, is given by the second line of Eq. (3.1) with the term ($\mathbf{q}=\mathbf{0}$) *excluded*. The subtracted tagged particle current $\mathbf{v}'$ in Eq. (2.2) has no component along the conserved total momentum $\mathbf{P}$. In the *unsubtracted* correlation function $\psi_N(t)$ in Eq. (2.3) the tagged particle current $\mathbf{v}$ does have a constant component $\mathbf{P}/N$. Hereafter, the results obtained through Eq. (3.1) are referred to as the finite N results of the extended mode-coupling theory [7].

In the thermodynamic limit ($V\to\infty$), all $O(N^{-1})$ terms disappear and the $\mathbf{q}$ sum in Eq. (3.1) is replaced by an integral over all $\mathbf{q}$ space. Evaluation yields the extended mode-coupling result for the infinite system:

$$\phi(t)=\frac{(1-f)v_0}{bfd(4\pi t)^{d/2}}\left[(d-1)\left[\frac{1}{D+\nu}\right]^{d/2}+\left[\frac{1}{D+\frac{1}{2}\Gamma}\right]^{d/2}{}_1F_1\left[\frac{d}{2},\frac{1}{2},-\frac{t}{t_s}\right]\right], \tag{3.2}$$

where v_0 is the volume of the unit cell of the space lattice on which the LGCA is defined. Apart from the overall factor $(1-f)$, the infinite system result (3.2) agrees with that of Ref. [7], where bf/v_0 is the *number of particles per unit volume*. In our discussion, we will be using the hydrodynamic relaxation times, t_s and t_v, for the combined damping effect of diffusion and sound modes, and for that of diffusion and shear modes, respectively, defined as

$$t_s=4(D+\tfrac{1}{2}\Gamma)/c_0^2,\quad t_v=4(D+\nu)/c_0^2\ . \tag{3.3}$$

For later purposes their numerical values are listed in Table I for a few typical models and densities. Furthermore, ${}_1F_1$ is the confluent hypergeometric function. The first term of Eq. (3.2) represents the shear-mode contribution $\phi^{\nu D}(t)$ and gives the leading long-time tail obtained in [2] (absent in the case of $d=1$) and the second one represents the subleading sound mode contributions. For *odd* values of the dimensionality d, the function ${}_1F_1$ decays exponentially, specifically, ${}_1F_1(\frac{3}{2},\frac{1}{2},-x)=(1-2x)e^{-x}$ in three dimensions. Hence the sound modes decays as $\exp(-t/t_s)$. For *even* values of d, the function ${}_1F_1$ cannot be expressed in elementary functions, and decays algebraically for large positive x, i.e., ${}_1F_1(d/2,\frac{1}{2},-x)\simeq(-1)^{d/2}(d-1)(2x)^{-d/2}$ for $d=2$ and 4. Hence, the sound mode contribution in (3.2) decays as t^{-d}, to be compared with $t^{-d/2}$ from the dominant shear-mode contribution.

Finally we remark that the constant term, $(1-f)/N$, can also be used as a finite-size correction to be applied to the computer simulations, i.e., $\phi_{\mathrm{MD}}(t)+(1-f)/N$ corresponds to $\phi_N(t)+(1-f)/N=\psi_N(t)$. The unrestricted $\mathbf{q}$ summation in (3.1) can be considered as a numerical approximation to the $\mathbf{q}$ integration, used to obtain (3.2). So $\psi_N(t)$ is the finite-N analog of the infinite system results. In comparing computer simulations with the infinite system result $\phi(t)$, we always apply the above finite-size correction, in order to collapse simulation data at different system sizes with the infinite system result.

TABLE I. The characteristic times for the two-dimensional FHP-III model and the three-dimensional FCHC model at several reduced densities. t_0, t_s, and t_v denote, respectively, the mean free time [Eq. (5.1)], the hydrodynamic relaxation time related to sound modes, and the one related to shear modes [Eq. (3.3)].

	2D FHP			3D FCHC		
f	t_0	t_s	t_v	t_0	t_s	t_v
0.05	5.7	26.9	29.3	1.79	14.5	16.8
0.1	2.8	13.4	14.4	0.97	7.6	6.2
0.25	1.1	5.6	5.9	0.49	3.8	4.2
0.4	0.7	3.8	4.0	0.37	3.0	3.2
0.75	0.3	3.0	3.3	0.24	3.3	3.7

IV. INTERFERENCE EFFECTS FROM REPLICAS

To interpret the physical phenomena and to discuss finite-size effects, it is instructive to transform the reciprocal-lattice sum in Eq. (3.1) back to a sum over the direct lattice using a formula from Fourier series,

$$L^{-d}\sum_{\mathbf{q}\in\mathcal{L}^*}\tilde{h}(\mathbf{q})=\sum_{l\in\mathcal{L}}h(lL)=\sum_{l\in\mathcal{L}}\frac{v_0}{(2\pi)^d}\int d\mathbf{q}\,\tilde{h}(\mathbf{q})e^{i\mathbf{q}\cdot l L}\ . \tag{4.1}$$

Here, $h(\mathbf{r})$ is a continuous function, defined in infinite space with a Fourier transform $\tilde{h}(\mathbf{q})=v_0^{-1}\int d\mathbf{r}\,h(\mathbf{r})\exp(-i\mathbf{q}\cdot\mathbf{r})$. The formula can be easily derived by Fourier transforming the periodic function $H(\mathbf{r})=\sum_{l\in\mathcal{L}}h(\mathbf{r}+lL)$. The formula is very useful if the inverse Fourier transform $h(\mathbf{r})$ of $\tilde{h}(\mathbf{q})$ can be calculated analytically. It is frequently used to convert slowly converging lattice sum in reciprocal space into a rapidly converging direct lattice sum and vice versa.

We first transform the shear-mode contribution $\psi_N^{vD}(t)$ in Eq. (3.1), where $\tilde{h}(\mathbf{q})=\exp(-\alpha q^2)$. With the help of (4.1) it can then be put into the equivalent form,

$$\psi_N^{vD}(t)=\frac{(d-1)(1-f)v_0}{dbf}\left[\frac{1}{4\pi(D+\nu)t}\right]^{d/2}\times\sum_l\exp\left[-\frac{l^2L^2}{4(D+\nu)t}\right]\ . \tag{4.2}$$

The lattice sums represent a superposition of an infinite number of Gaussians, centered at the origin of the system itself ($l=0$) and of all its periodic replicas at lL. As long as $\sqrt{4(D+\nu)t}\ll L$ or $t>t_v$, the sum in (4.2) is determined by the term with $l=0$, which represents the infinite system result in Eq. (3.2). As soon as $\sqrt{4(D+\nu)t}\simeq L$, the diffusive tails of the Gaussians from different replicas start to overlap and interference effects cause (4.2) to deviate from the infinite system result. In cases where one does not have a detailed theory for a finite system, simulations carried out for longer times will have little relevance for infinite system properties.

To convert the sound mode contributions $\psi_N^{\sigma D}(t)$ in (3.1) into a sum over the direct lattice, the inverse Fourier transform of $\tilde{h}(q)=\cos(\beta q)\exp(-\alpha q^2)$ is needed. In one dimension this is simply a shifted Gaussian. In general, the Fourier inversion can be carried out analytically for odd d values, but not for even ones. The result for the three-dimensional case is a shifted Gaussian, multiplied by a polynomial in t,

$$\psi_N^{\sigma D}(t)=\frac{(1-f)v_0}{3bf}\left[\frac{1}{4\pi(D+\frac{1}{2}\Gamma)t}\right]^{3/2}\times\left[{}_1F_1\left[\frac{3}{2},\frac{1}{2},-\frac{t}{t_s}\right]+\frac{1}{2}\sum_{l\neq 0}\frac{1}{lL}[E_l^{(-)}(t)+E_l^{(+)}(t)]\right]\ , \tag{4.3}$$

where $l=|\mathbf{l}|$ is the length of the lattice vector. The function $E_l^{(\pm)}$ is given as

$$E_l^{(\pm)}(t)=(lL\pm c_0t)\exp\left[-\frac{(lL\pm c_0t)^2}{4(D+\frac{1}{2}\Gamma)t}\right]\ . \tag{4.4}$$

This result has been derived in Ref. [7]. The first term in (4.3) gives the infinite system result and the sum with $\mathbf{q}\neq 0$ gives the contributions from the periodic replicas. Expression (4.3) represents a superposition of an infinite number of incoming wave packets $E_l^{(+)}$, and outgoing ones $E_l^{(-)}$, originating in every replica and traveling with the speed of sound. The contribution $E_l^{(+)}$ is very small compared to $E_l^{(-)}$.

In the one-dimensional case the factor $(lL\pm c_0t)$ is missing in $E_l^{(\pm)}(t)$. The term $E_l^{(-)}$ has a maximum at $t=lL/c_0=lt_a$, caused by sound waves from neighboring replicas reaching the system. Here the sound wave contribution $\psi_N^{\sigma D}(t)$ has equidistant maxima at multiples of the acoustic traversal time t_a.

In three dimensions the contribution $E_l^{(-)}(t)$ of outgoing sound waves is vanishing at $t=lt_a$ and it reaches a maximum and a minimum at t values, respectively, smaller and larger than lt_a. The locations of these extrema are obtained by solving a cubic equation. The maxima and minima in the three-dimensional case are, of course, not equidistant. There are in (4.3) for a simple-cubic lattice six nearest-neighbor sites with $l=1$ and twelve next-nearest-neighbor sites with $l=\sqrt{2}$, etc.

The width of the wave packets is increasing as $\sqrt{4(D+\frac{1}{2}\Gamma)t}$ due to diffusion of the tagged particle and due to the damping of sound waves. Strong interference effects due to sound waves from neighboring replicas occurs at times on the order of the acoustic traversal time, as has also been discussed in Refs. [7] and [8].

To carry out simulations on small systems that are free of interference effects from periodic boundary conditions, and have physical meaning for an infinite system, the following inequalities should be satisfied:

$$\sqrt{4(D+\tfrac{1}{2}\Gamma)t}\ll c_0t\ll L\quad\text{or}\quad t_s\ll t\ll t_a\ . \tag{4.5}$$

As t_s and t_v in Eq. (3.3) are of the same order (see Table I), the above criteria also guarantee the absence of interference effects from diffusive modes.

V. SIMULATIONS IN TWO DIMENSIONS

Here we study the 7-bit FHP-III model [15,2], which is defined on the triangular lattice. Particles can have six different velocities directed along the six directions of a triangular lattice, all with the same magnitude c. Moreover, a particle can have zero velocity. No two particles can be at the same site with the same velocity, so the maximum number of particles per site is seven. The dynamics of the tagged particle is defined in Ref. [2]. In our analysis we need the volume of the unit cell, $v_0=\sqrt{3}/2$, the speed of sound, $c_0=\sqrt{\frac{3}{7}}$, defined through $dbc_0^2=\sum_c c^2$, and the Boltzmann approximation to the sound damping constant, $\Gamma=\nu+\zeta$, with viscosities ν and ζ as calculated in Eq. (2.13) of Ref. [15]. In the same approximation, the VACF, the diffusion coefficient D, and the eigenvalue λ are given by [16]

$$\varphi_B(t)=(1-\lambda)^t\equiv\exp(-t/t_0)\ ,$$
$$D=c_0^2\left[\frac{1}{\lambda}-\frac{1}{2}\right]\ , \tag{5.1}$$
$$\lambda=1-(1-f)[1-(1-f)^{b-1}]/[(b-1)f]\ ,$$

with bit number $b=7$, the mean free time $t_0 = -1/\ln(1-\lambda)$, and f the reduced density. The values of t_0 are listed in Table I.

For this model, the *asymptotic* long-time tail is, according to Eq. (3.2), given by

$$\phi(t)=\frac{(1-f)v_0}{2bf}\left[\frac{1}{4\pi(D+\nu)t}\right]\equiv\frac{d_0}{t}\ . \tag{5.2}$$

In Ref. [2], the long-time tail of the VACF has been measured in computer simulations on *large systems* with $V=200\times200$ lattice sites for times $t\leq200$ at densities $f=0.1$ (0.1) 0.5 and with $V=500\times500$ for $t\leq500$ at $f=0.2$, 0.35, 0.5, and $f=0.75$. From the measured values of $t\phi_{\rm MD}(t)$, the coefficient d_0 has been extracted and the results have been compared with the mode-coupling result d_0 as a function of f. The agreement was within 5% as shown in Refs. [2] and [3]. However, the use of a more elaborate (self-consistent) theory gave almost perfect agreement within error bars [17].

The purpose of the present section is (i) to investigate the prediction of the full MC theory, which includes the subleading sound mode contributions Eq. (3.2), and (ii) to analyze the finite-size effects, manifesting themselves in the *time-independent* term $(1-f)/N$ in Eq. (2.4), and in the *interference* effects of sound waves arriving from periodic replicas of the system. Consequently, we will be studying smaller systems and shorter time intervals.

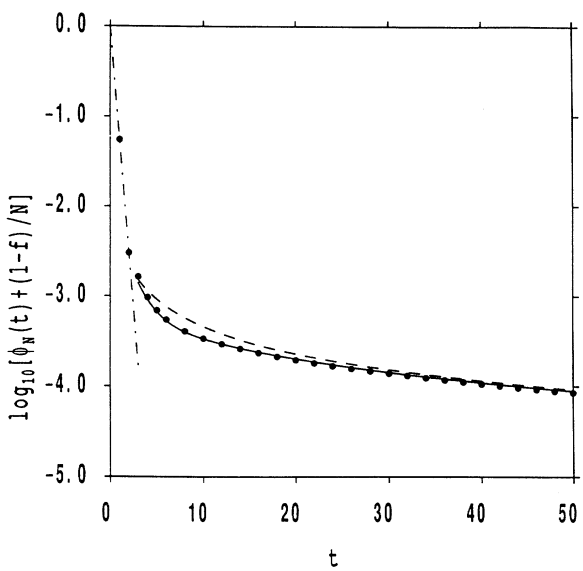

FIG. 1. The logarithm of the corrected velocity autocorrelation function $\psi_N(t)=\phi_N(t)+(1-f)/N$ vs time in the 2D FHP-III model. The system contains $V=100\times100$ lattice sites. The density, defined as the average number of particles per site per link, is $f=0.75$. The solid circles represent the results of computer simulations. Solid curve, prediction of the full mode-coupling (MC) theory for infinite systems [Eq. (3.2)]; short-dashed curve, prediction of the MC theory for finite-N systems [Eq. (3.1)]; the short-dashed curve is hidden under the solid curve; long-dashed curve, the asymptotic tail [Eq. (3.2)]. Note that the short-time simulation data agree with the Boltzmann approximation [Eq. (5.1)] (dashed-dotted line).

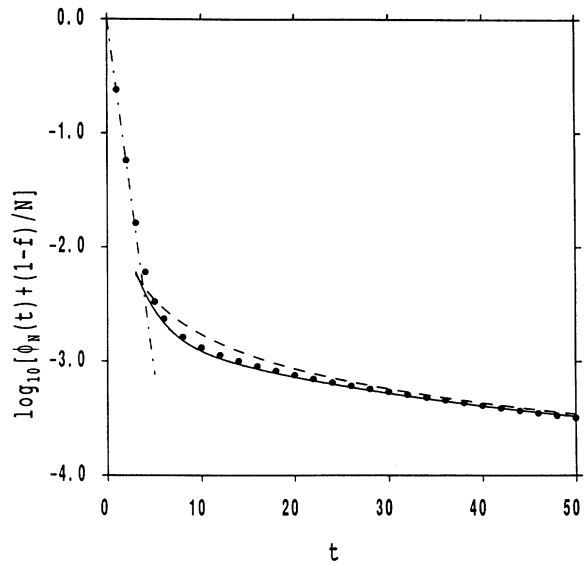

FIG. 2. As Fig. 1, but for system size $V=100\times100$ at density $f=0.40$.

Figures 1, 2, and 3 show the simulation data (solid circles), $\psi_{\rm MD}=\phi_{\rm MD}+(1-f)/N$, corrected for the constant $O(1/N)$ term in systems with $V=100\times100$ ($f=0.75$ and 0.4) and $V=50\times50$ ($f=0.1$) up to $t=50$. The error bars, denoting one standard deviation, are smaller than the size of the solid circles, except in Fig. 3. As explained in the Introduction, the moment propagation method does not have any statistical noise in the properties of the tagged particle, but does have statistical noise in the initial configurations of the N fluid particles, where N ranges from 10^3 to 10^6 in our two-dimensional simula-

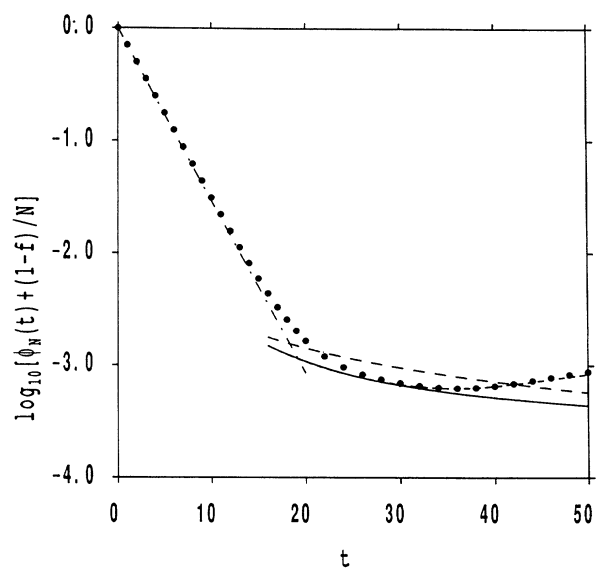

FIG. 3. As Fig. 1, but for system size $V=50\times50$ at density $f=0.10$. The acoustic traversal time for this system is $t_a=76$.

tions. This noise is measured by averaging typically over 10 different initial configurations of fluid particles.

At short times the VACF decays exponentially in agreement with Eq. (5.1) up to $t=15$, ($f=0.1$), $t=4$ ($f=0.4$), and $t=2$ ($f=0.75$), which corresponds to about $6t_0$. It should be noted that the Boltzmann approximation for time correlation functions in LGCA's is *exact* for $t=1,2$, provided the period of the macroscopic cell is larger than two lattice distances in every space direction (see also Sec. IV on the 3D FCHC model where this condition is not met).

For larger times we compare the data with the asymptotic and full MC theory for an infinite system. For densities $f=0.4$ and 0.75, the simulated data coincide with the asymptotic MC results (long-dashed line) for $t>20$ ($f=0.4$) and $t>25$ ($f=0.75$). More remarkably, the simulation data coincide within the error bars with the full MC theory (solid line) for $t>6t_0$. Here the kinetic theory ($t<6t_0$) and the full MC theory ($t>6t_0$) provide a quantitative description of the VACF.

By comparing the graphs of Figs. 3 and 4, referring to the same low-density measurements, we want to show several interesting points.

(i) There are strong finite-size effects. The MC theory for *finite systems* (short-dashed lines in Fig. 4) is in complete agreement with the simulations for $t>26$. The two distinct finite-size effects of the constant $O(1/N)$ term and of the interference effects will be discussed below.

(ii) The simulation results show *intermediate* behavior between kinetic relaxation ($t<6t_0$) and the full MC theory ($t>26\simeq 9t_0$).

(iii) Within the interval of 50 time steps, the asymptotic $1/t$ tail (long-dashed line) and the full MC theory (solid line) do not coincide because the *sound* mode contributions decay very slowly in two dimensions, like t^{-2}.

Consider first the constant $O(1/N)$ correction, which is important for comparing simulations from different system sizes, at least up to $t=\frac{1}{2}t_a$. In Fig. 3, we have compared the finite-N results $\psi_N=\phi_N+(1-f)/N$ with the corrected simulation data $\psi_{\rm MD}=\phi_{\rm MD}+(1-f)/N$. As a consequence, simulated data and finite system results can be collapsed with the infinite system results of the full MC theory, as shown in Fig. 3 for times $25<t<\frac{1}{2}t_a\simeq 38$, where $t_a=L/c_0$ is the acoustic traversal time. In Fig. 4, the *uncorrected* finite N prediction $\phi_N(t)$ and simulation data $\phi_{\rm MD}(t)$ are compared with the full MC theory for the infinite system. The purpose of showing the same data with and without the $(1-f)/N$ correction in Figs. 3 and 4 is to illustrate that without this correction there exists no time interval where infinite system predictions have any relationship to simulation data on small systems. The importance of this $O(1/N)$ correction for simulating infinite systems was already emphasized in our analysis of the VACF for a one-dimensional LGCA in Refs. [11] and [10].

The interference effects are caused by traveling sound waves, originating in periodic replicas. In Fig. 3, interference is noticeable for times larger than $\frac{1}{2}t_a\simeq 38$. To further elucidate the importance of both types of finite-size effects, we have performed simulations of high statistical accuracy on a system with $V=50\times 50$ ($t_a=76$) and $V=200\times 200$ ($t_a=305$) at density $f=0.75$, as shown in Figs. 5 and 6, respectively, for the uncorrected VACF $\phi_{\rm MD}(t)$. There is almost perfect agreement between the results from simulations and the full MC theory for finite systems (3.1). The dashed-dotted lines in

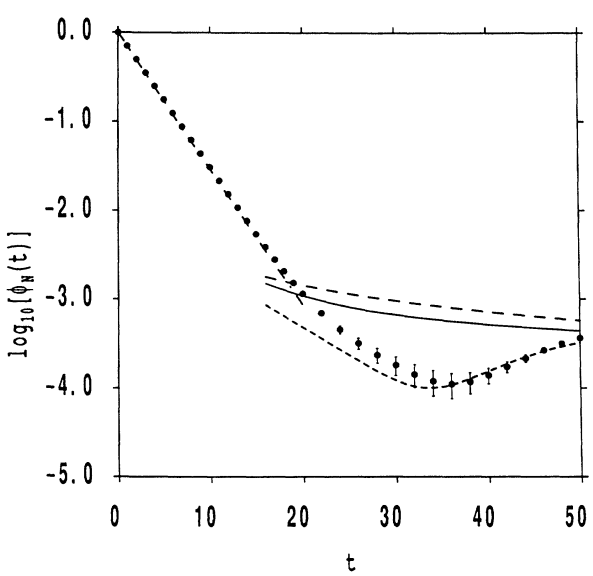

FIG. 4. As Fig. 3, but for the velocity autocorrelation function $\phi_N(t)$, that is, the velocity autocorrelation function *without* the finite-size correction $(1-f)/N$.

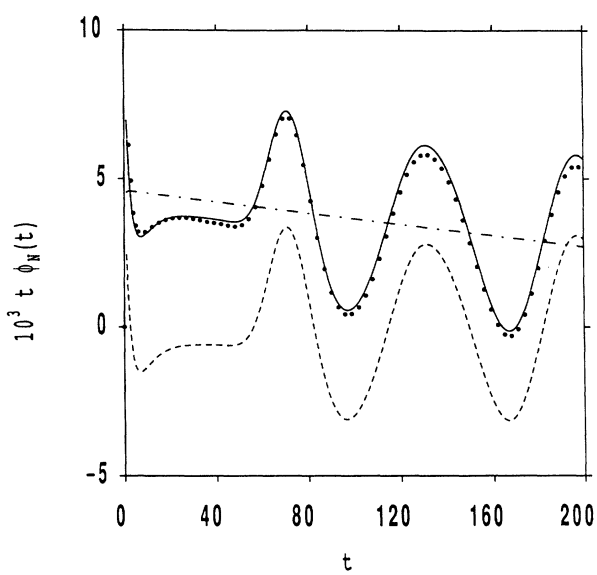

FIG. 5. $\phi_N(t)$ multiplied by time, vs time, in the 2D FHP-III model for system size $V=50\times 50$ at density $f=0.75$. The solid circles represent the results of computer simulations. The solid curve is the prediction of the full MC theory for finite systems, the dashed curve is only the sound mode contribution to this prediction, and the dashed-dotted line is only the shear-mode contribution (which is equal to the asymptotic tail). The acoustic traversal time is $t_a=76$.

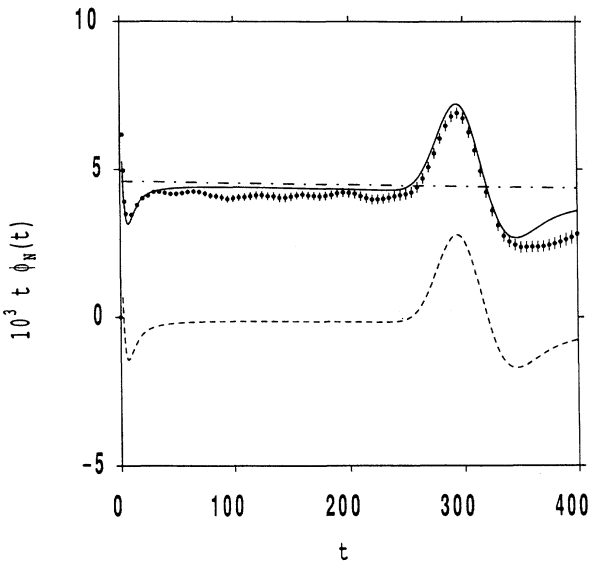

FIG. 6. As Fig. 5, but for system size $V=200\times200$ at density $f=0.75$. The acoustic traversal time for this system is $t_a=305$.

Figs. 5 and 6 show the shear-mode contributions, $t\phi_N^{\nu D}\simeq d_0-t(1-f)/N$. This is essentially a straight line because the interference effects in Eq. (4.2) of the purely diffusive νD modes in neighboring replicas are of order $\exp[-L^2/4(D-\nu)t]\sim10^{-4}$ (Fig. 5 at $t\simeq200$) and 10^{-34} (Fig. 6 at $t\simeq400$), and completely negligible for the present systems.

In two dimensions we do not have an explicit real-space representation of the sound mode contributions, such as (4.3). Nevertheless, most features in Figs. 5 and 6 can be understood in a quantitative manner. The dashed lines show the contributions from the sound modes and the solid lines show the sum of both previous contributions. The first maximum occurs at the acoustic traversal time ($t_a=76$ in Fig. 5 and $t_a=305$ in Fig. 6) and the width of the peaks is determined by $\sqrt{4(D+\frac{1}{2}\Gamma)t}$. The second maximum in Fig. 5 occurs at $\sqrt{3}t_a\simeq132$, which corresponds to sound waves arriving from next-nearest-neighbor replicas. The maxima originate from Gaussian wave packets, excited in neighboring replicas, that travel with the speed of sound and broaden as $\sqrt{4(D+\frac{1}{2}\Gamma)t}$ due to diffusion and damping of the sound waves.

We have also verified that the diffusion coefficient calculated from the simulation data with help of Eq. (2.1) and summed to an upper limit t_M with $T_M>\{t_s,t_v\}$ is practically equal to the Boltzmann value as given in Eq. (5.1).

Before concluding this section on the long-time behavior of the FHP-III model, we recall that the MC theory in two dimensions is not an internally consistent theory. On the one hand, it predicts that the long-time tail $\simeq1/t$ would lead to *diverging* transport coefficients, e.g., $D(t)=\int^t dt/t\rightarrow\ln(t)$ for $t\rightarrow\infty$. On the other hand, the coefficient d_0 in (3.1) is determined by the *finite* short-time Boltzmann values of the transport coefficients. Recently two of us [17] performed simulations for the FHP model at $f=0.7$, 0.75, and 0.8 for $t\leq1800$ in systems with $V=2000\times2000$ sites. For such superlong time intervals, a faster than $1/t$ decay has been observed and explained quantitatively with the help of a self-consistent MC theory [17,18].

VI. SIMULATIONS IN THREE DIMENSIONS

The quasi-three-dimensional FCHC model is contained in a macroscopic periodicity cell that is a four-dimensional slab with a volume of $2L^3$, i.e., two-lattice-spacings wide in the fourth dimension. It is defined on the *even sublattice* $\{r_x+r_y+r_z+r_t=\text{even}\}$ of a four-dimensional simple-cubic lattice and contains, therefore, $V=L^3$ accessible sites. There are $b=24$ allowed velocities per site, specified by the next-nearest-neighbor lattice vectors: $(\pm1,\pm1,0,0)$, $(\pm1,0,\pm1,0)$, $(\pm1,0,0,\pm1)$, $(0,\pm1,\pm1,0)$, $(0,\pm1,0,\pm1)$, $(0,0,\pm1,\pm1)$. The FCHC model may also be interpreted as a strictly three-dimensional model [1], defined on a simple-cubic lattice where all $V=L^3$ sites are accessible. The six nearest-neighbor links may be doubly occupied (by distinguishable particles) and the twelve next-nearest-neighbor links are at most singly occupied.

The speed of sound is given by $c_0^2=(4b)^{-1}\sum_c c^2=\frac{1}{2}$. The kinematic viscosity ν and diffusion coefficient D are determined by the four-dimensional collision rules and have been calculated in [3] for the relevant version of the FCHC model within the approximation of uncorrelated collisions based on the Boltzmann approximation. The sound damping constant is equally determined by the four-dimensional collision rules, and given by $\Gamma=\frac{3}{2}\nu$, since the bulk viscosity ζ vanishes for the single speed FCHC model. It was also shown recently [16] that the Boltzmann approximation to the VACF and the diffusion coefficient for the tagged particle in *all versions* of the FCHC model are given by (5.1) with $b=24$. The mean free time t_0, defined in (5.1) and listed in Table I, is rather short for this model. Even at a density of $f=0.1$, a particle suffers a collision at every time step because there are on the average 2.4 particles present per site. For this model the asymptotic long-time tail in the thermodynamic limit is given by (5.2) with $d=3$, i.e.,

$$\phi(t)=\frac{2(1-f)}{3bf}\left[\frac{1}{4\pi(D+\nu)t}\right]^{3/2}\equiv d_0t^{-3/2}\,, \qquad (6.1)$$

where the volume of the unit cell $v_0=1$. In the computer simulations of [3] the tail in $t^{3/2}\phi(t)$ has been measured in a system with $V=60^3$ sites at densities ranging from $f=0.1$ to 0.9. The results have been compared with the MC results and were found to be in excellent agreement with the asymptotic tail (6.1) of the MC theory.

Before comparing the three-dimensional simulation data with the MC results, we discuss the short-time behavior of the VACF in at densities $f=0.1$, 0.4, and 0.75. Here the VACF decays exponentially and is correctly given by the Boltzmann approximation up to $t\simeq6t_0$, just like in the two-dimensional case. In Sec. IV it was mentioned that the Boltzmann approximation for the VACF

is still exact at $t=2$ for all lattice-gas models in a sufficiently large macroscopic box. Here this is no longer true due to the narrow four-dimensional slab containing the FCHC fluid. The short spatial period two of this slap induces extra velocity correlations at $t=2$, so that the assumption of uncorrelated collisions, basic to the Boltzmann approximation, is violated. In the simulations of Ref. [3] the measured value of $\phi_{\rm MD}(2)$ was larger than the Boltzmann values by less than 2% at $f=0.15$ and is increasing to about $\phi_{\rm MD}(2)\simeq 2\phi_B(2)$ at $f=0.8$. These velocity correlations are not of dynamic, but rather of geometric origin, and are related to the period two in the fourth spatial direction. This interpretation was recently confirmed [12] in computer simulations on the FCHC model, where the VACF was measured in a real four-dimensional system of L^4 sites and where the relation $\phi_{\rm MD}(2)=\phi_B(2)$ was verified. Although $\phi(2)$ might differ from its Boltzmann value, the diffusion coefficient D, as calculated from the simulation data using (2.1), is essentially equal to the Boltzmann value in (5.1).

Next we turn to the MC theory. In Figs. 7–10, the MC results for the infinite systems are compared with the corrected simulation results at densities $f=0.1$, 0.25, 0.5, and 0.75, respectively. The simulation data for the VACF for times $t<L$ (with $L=50$, 40, 30, and 60, respectively) are within one standard deviation from the asymptotic tails (long-dashed lines) for t larger than 20, 6, 5, and 4, respectively. Note that all simulations involve at least 3×10^5 particles. Including sound modes (solid lines) deteriorates the agreement. The sound modes

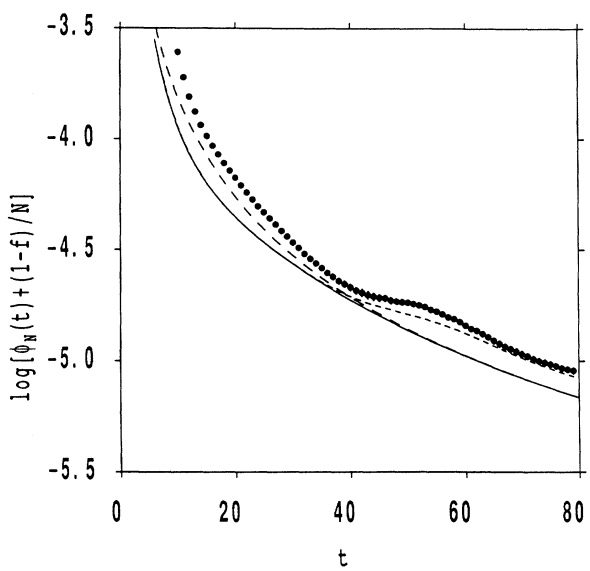

FIG. 7. The logarithm of the corrected velocity autocorrelation function $\psi_N(t)=\phi_N(t)+(1-f)/N$ vs time in the 3D FCHC model. The system size is $V=50\times50\times50$, the density is $f=0.10$. The solid circles represent the results of computer simulations. Solid curve, prediction of the full MC theory for infinite systems [Eq. (3.2)]; short-dashed curve, prediction of the MC theory for finite-N systems [Eq. (3.1)]; long-dashed curve, the asymptotic tail [Eq. (6.1)]; for shorter times, the short-dashed curve coincides with the solid curve.

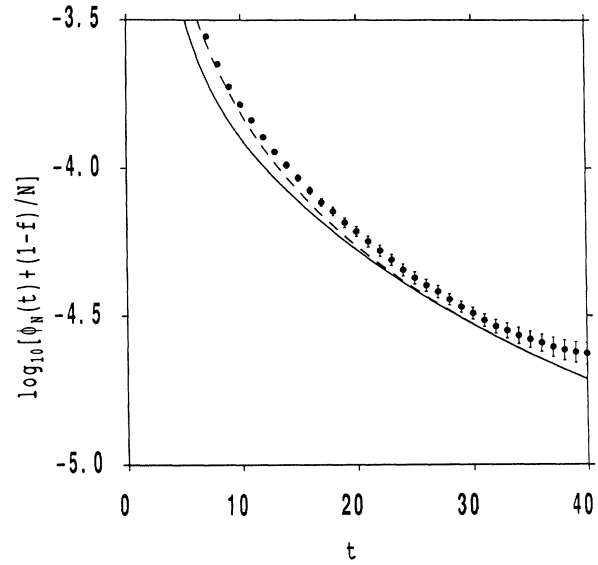

FIG. 8. As Fig. 7, but for system size $V=40\times40\times40$ at density $f=0.25$.

in Eq. (3.2) are described by ${}_1F_1(\frac{3}{2},\frac{1}{2},-t/t_s)=\exp(-t/t_s)(1-2t/t_s)$, where the hydrodynamic relaxation time t_s is listed in Table I. The full MC theory and the simulations agree within one standard deviation only after the longer times 30, 20, 18, and 20, respectively. These results seem to suggest that the FCHC fluid exhibits intermediate dynamic behavior in between the kinetic relaxation, described by the Boltzmann approximation, and the hydrodynamic relaxation, described by the MC theory.

In Figs. 11–13, we study interference effects of sound

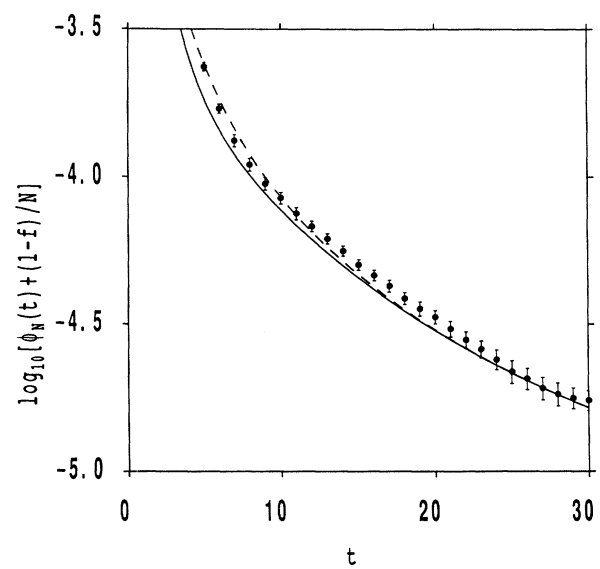

FIG. 9. As Fig. 7, but for system size $V=30\times30\times30$ at density $f=0.50$.

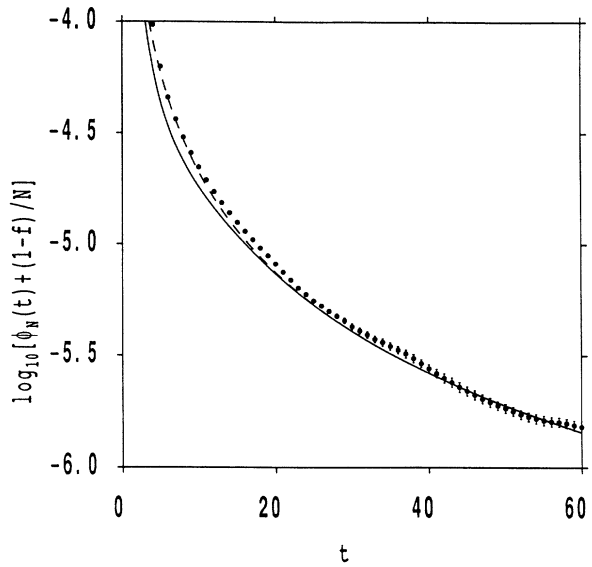

FIG. 10. As Fig. 7, but for system size $V=60\times60\times60$ at density $f=0.75$.

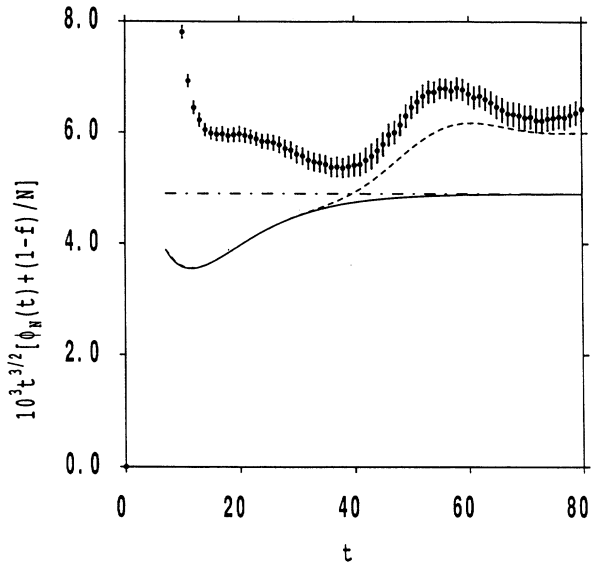

FIG. 12. As Fig. 11, but for system size $V=50\times50\times50$ at density $f=0.10$. The acoustic traversal time is $t_a=71$.

waves from neighboring replicas in small systems using Eq. (4.3). The figures show the VACF, $\psi_N=\phi_N+(1-f)/N$, corrected for the constant $O(1/N)$ term of Eq. (2.4) at densities $f=0.4$ ($V=30^3, t_a=L/c_0\simeq42$), $f=0.1$ ($V=50^3, t_a\simeq71$), and $f=0.05$ ($V=50^3, t_a=71$), respectively. The dashed-dotted line represents the asymptotic $t^{-3/2}$ tail, the solid line the full MC theory for an infinite system, and the dashed line the finite-N results. Finite and infinite system results start to differ at $t\simeq25$, 35, and 25, respectively. These differences have only statistical significance in Fig. 12 ($N=3\times10^5$) and Fig. 13 ($N=1.5\times10^5$) and follow the trends of the finite-N results. At times 40, 60, and 80, the simulation data exceed the theoretical results at finite N by, respectively, 8%, 8%, and 6% in Fig. 12 ($f=0.1$) and by, respectively, 40%, 26%, and 9% in Fig. 13 ($f=0.05$). These figures definitely show the importance of the finite-size correction $(1-f)/N$ and of the interfer-

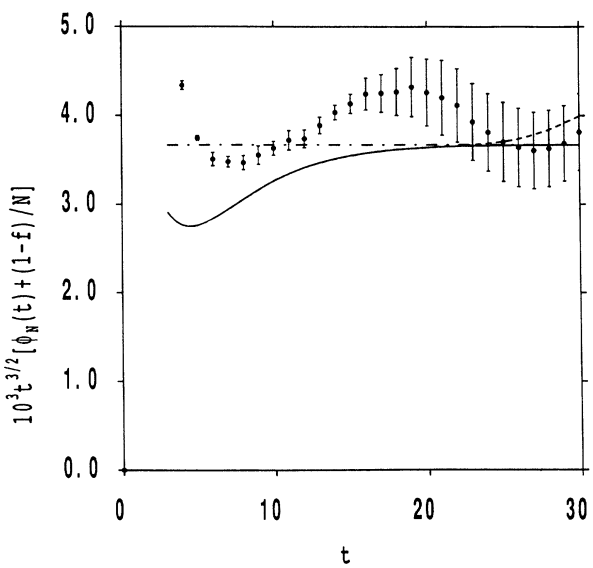

FIG. 11. $\psi_N(t)$ multiplied by $t^{3/2}$, vs time, in the 3D FCHC model for system size $V=30\times30\times30$ at density $f=0.40$. The solid circles represent the results of computer simulations. Solid curve, prediction of the full MC theory for infinite systems; dashed curve, finite-N result; dash-dotted curve, the asymptotic tail [Eq. (6.1)]. The acoustic traversal time is $t_a=42$.

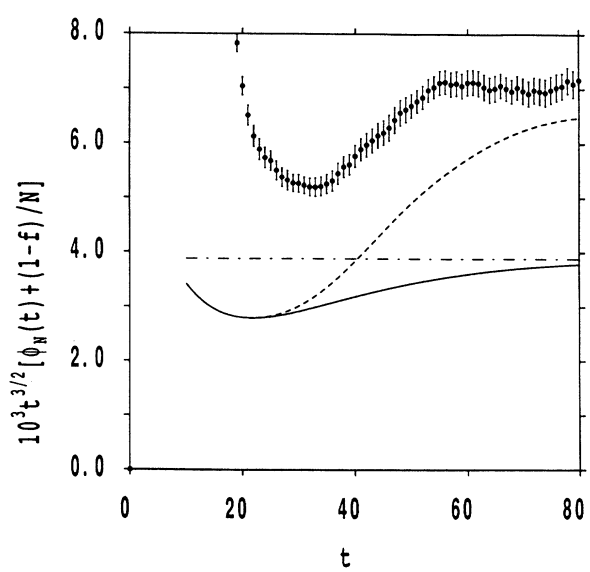

FIG. 13. As Fig. 11, but for system size $V=50\times50\times50$ at density $f=0.05$. The acoustic traversal time is $t_a=71$.

ence effects of sound modes, since the infinite system results are about 22% (Fig. 12) and 43% (Fig. 13) smaller than the simulation data at the largest times. In Figs. 7–10 the differences between the corrected VACF, $\phi_N(t)+(1-f)/N$, and its infinite system limit $\phi(t)$ are invisibly small.

In three dimensions there is no simple relationship between maxima in $t^{3/2}\phi_N(t)$ and the acoustic traversal time. The theoretical analysis of (4.3) shows destructive interference at times $t=t_a$ of the sound waves from different replicas. Furthermore, the widths of positive and negative peaks are very large in the smallest systems, since the hydrodynamic relaxation times t_s and t_v in Eq. (3.3) become comparable to t_a, and the peaks in (4.3) cannot be resolved.

We also point out that the appearance of sizable finite-size effects due to interfering sound waves can only occur after $\frac{1}{2}t_a \simeq 21$ and 35, respectively, as is the case in Figs. 11 and 12. The fact that in Fig. 13 differences between finite and infinite systems occur already at $t \simeq 25 < \frac{1}{2}t_a$ indicates that the hydrodynamic concepts of interfering sound waves break down at low densities ($f=0.05$) and small system sizes ($L=50$) at short times. This is corroborated by the violation of the inequalities (4.5). It implies that the spreading $\sqrt{4(D+\frac{1}{2}\Gamma)t} \simeq 15$ of the wave packets through damping and diffusion is comparable to the propagation distance $c_0 t \simeq 17$ for the relevant times and system sizes (here $L=50$).

In concluding the analysis of the three-dimensional simulations, we recall that there are indications for long-lived intermediate time behavior. A quantitative explanation of this intermediate dynamics probably requires a more sophisticated kinetic theory that takes into account correlated collision sequences, more complicated than the simple ring collisions contained in the MC theories. Furthermore, we cannot exclude that the quasi-three-dimensional and four-dimensional FCHC model has some hidden spurious invariants, which might explain both the observed long-lived intermediate behavior, as well as the deviations between theory and simulations at larger times in smaller systems.

VII. CONCLUSION

This paper is the lattice-gas counterpart of the computer studies of Erpenbeck and Wood [7,8] on measuring long-time behavior of the VACF in hard sphere and hard disk systems and on comparing it with the mode-coupling (MC) theory for *finite* systems. The two models considered here are the two-dimensional FHP model, defined on the triangular lattice [1], and the quasi-three-dimensional FCHC model, which is defined, in its three-dimensional interpretation, on a simple-cubic lattice [1].

The extended mode-coupling theory for finite systems not only includes the dominant shear modes of fluids, yielding $t^{-d/2}$ tails, but also subleading sound mode contributions, that decay in even dimensions like t^{-d} and in odd dimensions exponentially with a hydrodynamic relaxation time $t_s=4(D+\frac{1}{2}\Gamma)/c_0^2$. The sound modes produce strong interference effects through the periodic boundary conditions and cause large deviations from the infinite system results. It is shown here for two- and three-dimensional CA fluids, and in Ref. [11] for a one-dimensional CA fluid, that the extended MC theory for finite systems gives, in one and two dimensions excellent, and in three dimensions good to reasonable agreement with extensive computer simulations on small ($N \simeq 10^3$) and large ($N \simeq 10^6$) systems.

At the end of Sec. III and in the discussion of the simulation data in Sec. V, we have emphasized the importance of the finite-size correction term $(1-f)/N$ for collapsing simulation data of different system sizes with the theoretical predictions for infinite systems, at least for times less than half the acoustic traversal time. It is particularly important in cases where no detailed theoretical analysis can be made of the interference effect of sound waves in small systems, coming from neighboring replicas, and where only theoretical predictions for the infinite system are available. Our analysis shows that one should discard in that case the simulation data for times exceeding half the acoustic traversal time.

In one and two dimensions, the excellent agreement sets in at about 9 mean free times t_0. Figures 4 and 5 show the importance of finite-size effects caused by interference of sound waves from periodic replicas of the system. As Boltzmann relaxation $\exp(-t/t_0)$ essentially holds for $t \le 6t_0$ (see Figs. 1–4 for two dimensions), one has in practice a quantitative theory of the VACF in two-dimensional CA fluids. This result confirms the validity of hydrodynamic concepts down to rather small spatial and temporal scales.

In three-dimensional systems the asymptotic tail of the VACF $d_0 t^{-3/2}$ is in good agreement with the computer simulations, but it only sets in after a rather long times ranging from $150t_0$ (see Fig. 7 with $f=0.1$) to $60t_0$ (see Fig. 10 with $f=0.75$). Inclusion of the sound modes does not extend the validity of the theory to shorter times (as was the case in two dimensions). There exists a large region of unexplained intermediate time behavior.

Higher-order mode-coupling contributions produce in three dimensions an infinite series of subleading asymptotic correction terms, decaying like $t^{-\alpha_n}$ with $\alpha_n = 2-2^{-n}$ ($n=1,2,\ldots$) (for a recent review, see Ref. [4]). We have numerically evaluated these contributions and found them to be totally negligible.

Interference effects of sound waves from neighboring replicas in three-dimensional systems have only been observed at the *lowest* densities ($f=0.1$ in Fig. 12 and $f=0.05$ in Fig. 13). The simulations on these low-density systems follow the trends of the MC predictions only rather slowly (after about one acoustic traversal time) and show deviations from the finite-N results of less than 10%. As expected, the infinite system results have little relevance for the low-density simulation data.

The poor agreement of the MC theory and the simulations in the three-dimensional FCHC fluid at the lowest densities is somewhat unexpected in view of the excellent agreement in the one- and two-dimensional simulations. In fact, in recent simulations [12] of a four-dimensional version of the FCHC model on a system with $V=30^4$ sites, the long-time part of the VACF has been measured

and compared with the rather weak asymptotic tail $d_0 t^{-2}$ in Eq. (3.2). In the density range $0.4 < f < 0.8$ the measured exponent was 2.035 ± 0.043 and the value of d_0 was about 20–30% larger than the theoretical value. For densities outside this interval the deviations are larger.

The observed long-lived intermediate behavior and the observed deviations between theory and simulations in the asymptotic tails in the three- and four-dimensional FCHC model might indicate the presence of a hidden spurious invariant.

ACKNOWLEDGMENTS

T. N. thanks the Institute of Theoretical Physics of the University of Utrecht for its kind hospitality during his stay. The work of the FOM Institute is part of the scientific program of FOM and is supported by "Nederlandse Organisatie voor Wetenshappelijk Onderzoek" (NWO). Computer time on the NEC-SX2 at Nationaal Lucht-en Ruimtevaart-kundig Laboratorium was made available through a grant by NFS (National Fonds Supercomputers).

*On leave of absence from Senshu University, Higahi-mita, 2-1-1, Tama-Ku, Kawasaki 214, Japan.

[1] U. Frisch, B. Hasslacher, and Y. Pomeau, Phys. Rev. Lett. **56**, 1505 (1986); U. Frisch, D. d'Humières, B. Hasslacher, P. Lallemand, Y. Pomeau, and J. P. Rivet, Complex Systems **1**, 649 (1987).

[2] D. Frenkel and M. H. Ernst, Phys. Rev. Lett. **63**, 2165 (1989).

[3] M. A. van der Hoef and D. Frenkel, Phys. Rev. A **41**, 4277 (1990); Physica D **47**, 191 (1991).

[4] M. H. Ernst, Physica D **47**, 198 (1991).

[5] M. H. Ernst and J. W. Dufty, J. Stat. Phys. **58**, 57 (1990).

[6] T. Naitoh, M. H. Ernst, and J. W. Dufty, Phys. Rev. A **42**, 7187 (1990).

[7] J. J. Erpenbeck and W. W. Wood, Phys. Rev. A **26**, 1648 (1982).

[8] J. J. Erpenbeck and W. W. Wood, Phys. Rev. A **32**, 412 (1985).

[9] M. H. Ernst, E. H. Hauge, and J. M. J. van Leeuwen, Phys. Rev. A **4**, 2055 (1971).

[10] T. Naitoh, M. H. Ernst, M. A. van der Hoef, and D. Frenkel, in *Proceedings of the KSLA Workshop, Numerical Methods for Simulation of Multiple-Phase and Complex Flow, Amsterdam, 1990,* edited by T. Verheggen, Springer Lecture Notes in Physics (Springer, Berlin, in press); T. Naitoh and M. H. Ernst, in *Proceedings of the Euromech Colloquium Vol. 267, Discrete Models of Fluid Dynamics, Coimbra, Portugal,* edited by A. S. Alves, Series on Advances in Mathematics for Applied Sciences (World Scientific, Singapore, in press).

[11] T. Naitoh, M. H. Ernst, M. A. van der Hoef, and D. Frenkel (unpublished).

[12] M. Dijkstra and M. A. van der Hoef (unpublished).

[13] M. S. Green, Phys. Rev. **119**, 829 (1960).

[14] J. L. Lebowitz and J. K. Percus, Phys. Rev. **122**, 1075 (1961); J. L. Lebowitz, J. K. Percus, and L. Verlet, *ibid.* **153**, 250 (1967).

[15] D. d'Humières and P. Lallemand, Complex Systems **1**, 599 (1987).

[16] M. H. Ernst and T. Naitoh, J. Phys. A (to be published).

[17] M. A. van der Hoef and D. Frenkel, Phys. Rev. Lett. **66**, 1591 (1991).

[18] J. A. Leegwater and G. Szamel (unpublished); J. A. Leegwater, Ph.D. thesis, University of Utrecht, 1991.